NATIONAL ADVISORY COMMITTEE FOR AERONAUTICS

TECHNICAL NOTE

No. 1216

EFFECTS ON PERFORMANCE OF CHANGING THE DIVISION OF WORK BETWEEN INCREASE OF ANGULAR VELOCITY AND INCREASE OF RADIUS OF ROTATION IN AN IMPELLER

By Ambrose Ginsburg, William K. Ritter and John Palasics

Aircraft Engine Research Laboratory
Cleveland, Ohio

Washington
February 1947

NATIONAL ADVISORY COMMITTEE FOR AERONAUTICS

TECHNICAL NOTE NO. 1216

EFFECTS ON PERFORMANCE OF CHANGING THE DIVISION OF WORK BETWEEN INCREASE OF ANGULAR VELOCITY AND INCREASE OF RADIUS OF ROTATION IN AN IMPELLER

By Ambrose Ginsburg, William K. Ritter
and John Palasics

SUMMARY

The effect on the performance of increasing the angular velocity of an impeller and consequently increasing the amount of work of compression resulting from the angular acceleration of the air in the impeller was investigated for four impellers in combination with a vaneless diffuser in a variable-component supercharger test rig over a range of actual tip speeds from 800 to 1300 feet per second. Impellers A, B, and C were also tested at two constant impeller angular velocities.

Impellers A, B, and C consisted of radial-bladed sections with the same inducer section. Impellers B and C were made by reducing the discharge-tip diameter of impeller A (12-in. diameter) to 10.76 inches (impeller B) and to 9.52 inches (impeller C). Impeller D consisted of the inducer section without a radial-bladed section.

When the amount of work resulting from the angular acceleration was increased with respect to the work of compression resulting from the increased radius of rotation of the impeller, the impeller adiabatic efficiency, pressure coefficient, and volume-flow capacity were improved. The volume-flow capacity of the impeller was independent of impeller diameter and impeller tip speed but dependent upon the impeller angular velocity. The relation between maximum volume flow and impeller angular velocity was linear. The flow restriction that limits the volume-flow capacity of the compressor existed in the inducer section. The flow was restricted when a critical pressure drop occurred in the inducer section. With an increased impeller blade-inlet relative Mach number, the negative blade-inlet angles of attack at which the critical pressure drop occurred decreased. Any detrimental effects on impeller performance resulting from transonic velocities relative to the impeller

inlet blade tip were small as compared with the desirable performance effects obtained by increasing the impeller angular velocity.

INTRODUCTION

The ideal work of compression in a centrifugal-type impeller consists of two types of energy addition: one by the angular acceleration of the air and the other by increased air velocities resulting from an increased radius of rotation. The process of accelerating the air to the angular velocity of the impeller is sometimes called the inducer function. The acceleration of the air produced by the increased radius of rotation is called the Coriolis acceleration. The two accelerations represent two different types of air flow in the impeller. The angular acceleration produces a pressure rise by diffusion of the dynamic pressure of the relative velocity in the impeller passage. The Coriolis acceleration produces a pressure rise as a result of centrifugal force without any diffusion.

In an impeller, the inducer function may be physically separated from the Coriolis acceleration as in reference 1 or the two accelerations may be partly or entirely overlapping. Conventional impellers are designed to have most of the work of compression done by the Coriolis acceleration and to have very little or no overlapping of the angular and Coriolis accelerations. The reason for such an arrangement is that the angular acceleration of air in a centrifugal-type impeller is generally believed to be an inefficient process. Moreover, the low ratio of impeller inlet-tip to discharge-tip diameters needed to increase the ratio of Coriolis to angular acceleration provides low Mach numbers at the impeller inlet, a condition considered necessary for satisfactory impeller performance. The merits of the conventional method of impeller loading, however, are not obvious. An increase in angular velocity may be more effective in adding energy in the impeller than the conventional method, for the flow phenomena in the impeller passage are incompletely known.

The effect on performance obtained by increasing the amount of work of compression resulting from the angular acceleration of the air in the impeller has been investigated at the NACA Cleveland laboratory. Four impellers were tested in a variable-component supercharger test rig over a range of actual impeller tip speeds from 800 to 1300 feet per second. Impellers A, B, and C were also tested at two constant impeller angular velocities. Impellers A, B, and C consisted of radial-bladed sections with the same inducer section. Impellers B and C were made by reducing the discharge-tip diameter of impeller A (12 in.) to 10.76 and 9.52 inches, respectively.

Impeller D consisted of the inducer section without any radial-bladed section. This inducer section, because of the profile of its air-flow passages, imparted a Coriolis acceleration to the air in addition to its primary function of imparting angular velocity to the entering air.

The adiabatic efficiency, the pressure coefficient, and the volume flow of the four impellers are compared. An analysis of the volume-flow limitations of the compressor is presented that indicates what part of the compressor system limits the volume-flow capacity and shows the nature of the flow restriction. The use of impeller blade-inlet relative Mach number as an impeller design parameter is discussed.

IMPELLERS

The four impellers used in the investigation are shown in profile view in figure 1. Impellers A, B, and C consisted of radial-bladed impeller sections with the same inducer section. Impellers B and C were made by successive reductions in the tip diameter of the radial-bladed section of impeller A. Impeller D consisted of the inducer section without a radial-bladed impeller section.

As shown by figure 2, impeller A had 18 blades and consisted of the inducer section and a 12-inch-diameter radial-bladed section. The passage area normal to the mean-flow path in both the inducer section and in the radial-bladed section was held constant by selection of the shroud profiles. Impeller B had a tip diameter of 10.76 inches and impeller C had a tip diameter of 9.52 inches. For these two diameter reductions only the blades were removed; the impeller rear shroud was left to serve as part of the diffuser rear wall. Impeller D, which consisted of only the inducer section, was obtained by the removal of all the blades of the impeller radial-bladed section. The impeller rear shroud again served as the diffuser rear wall. A photograph of the inducer section, impeller D, is shown in figure 3.

The inducer section was single stage and designed to impart solid-body, or wheel, rotation to the entering air at constant angular acceleration along the axial depth. The design of this type of inducer section is described in reference 2. The inducer section had 18 blades, an inlet-tip diameter of 8 inches, an inlet-hub diameter of 2.85 inches, a discharge-tip diameter of 9.52 inches, and a discharge-hub diameter of 6.39 inches. In order to maintain passage-area control through the inducer section and also to avoid

any abrupt change in curvature of the flow path at the junction of the inducer section and the radial-bladed impeller section, the shroud profiles of the inducer section were not at constant radius along the axial depth of the inducer section. The inducer section had an axial depth of 2.45 inches and a design load coefficient of 0.294 cubic foot per revolution.

Comparative design information for the four impellers is given in the following table:

Impeller	Impeller tip diameter (in.)	Ideal work of compression in impeller	
		Resulting from angular acceleration (percent of total)	Resulting from Coriolis acceleration (percent of total)
A	12.00	22	78
B	10.76	27	73
C	9.52	35	65
D	[a]9.52	49	51

[a]Tip diameter varies from 9.52 inches to 6.39 inches.

The Coriolis acceleration occurred in the inducer section (impeller D) because of the increase of the radius of rotation through the flow passage. The work of compression occurring in the radial-bladed sections of impellers A, B, and C resulted entirely from the Coriolis acceleration of the air imparted by the increasing radius of rotation. For these four impellers, the ratios of the ideal work of compression resulting from the angular and Coriolis accelerations remained constant for a given impeller tip diameter irrespective of impeller tip speed.

APPARATUS AND TEST PROCEDURE

Test setup. - The four impellers were investigated in combination with a vaneless diffuser in a variable-component supercharger test rig. The vaneless diffuser was 34 inches in diameter and its design was similar to that of diffusers which in previous tests

had shown good pressure conversion over a wide range of operating conditions. The variable-component supercharger test rig was as described in reference 3 except that a flat-plate front collector cover was used to simplify instrument installation. The impellers were driven by an aircraft engine in conjunction with a speed-increaser gear.

Instrumentation. - Temperature and pressure measurements were made according to the standards recommended in references 3 and 4 whenever applicable. All air temperatures were measured with calibrated iron-constantan thermocouples and a potentiometer. Total pressures in the inlet and outlet pipes were measured with pressure tubes of 0.093-inch outside diameter and 0.067-inch bore. Static wall taps of 0.020-inch bore were used in the inlet and outlet pipes. Static pressures were taken along the impeller stationary shroud (see fig. 1) using static wall taps of 0.020-inch diameter. Total-pressure survey tubes were installed in the diffuser as shown in figure 1. Total pressures were read at the midpoint between the diffuser walls and at 0.063 inch from each wall by a tube 0.10 inch in diameter with a 0.020-inch-diameter hole drilled in its side.

Air flow and air pressure were regulated by butterfly throttle valves in both the inlet and outlet pipes. A large orifice tank with a thin-plate orifice at the entrance was used to measure the quantity of air entering the impeller. (See reference 5.)

The desired constant speed was maintained with a speed strip and a stroboscopic light operated on 60-cycle current and checked with an electric counter and a stop watch.

Test procedure. - The impellers were investigated according to the procedure recommended in references 3 and 4 whenever applicable. All runs were made with ambient inlet air. For each constant tip speed, the volume flow was varied in a number of steps from wide-open throttle to surging, except at the flow cut-off point for the higher tip speeds, where insufficient driving power necessitated a small closure of the inlet throttle before the desired speed could be obtained. At the flow cut-off the maximum volume flow through the impeller was inappreciably affected by a small reduction in mass flow. For all throttle settings except wide-open throttle, a constant outlet total pressure of 10 inches of mercury above atmospheric pressure was maintained with impellers A, B, and C. With impeller D, the outlet total pressure was maintained at 3 inches of mercury above atmospheric pressure.

Runs were made over an actual impeller-tip-speed range of 800 to 1300 feet per second for impellers A and B. (All impeller tip speeds in this report are actual unless otherwise noted.) Impeller C was limited in speed to 1200 feet per second by the available driving power. No runs were made of impeller D above an impeller tip speed of 1000 feet per second because of possible mechanical failure of the inducer blades at higher speeds.

Impellers A, B, and C were also investigated at two constant angular velocities. The following table shows the relation of angular velocity and impeller tip speed for the three impellers:

Impeller	Angular velocity (radians/ sec)	Impeller tip speed (ft/sec)
A	2000	1000
B		897
C		793
A	2400	1200
B		1076
C		952

COMPUTATIONS

Computations of over-all adiabatic efficiency η_{ad} and pressure coefficient q_{ad} for the unit composed of the impeller, the vaneless diffuser, and the variable-component supercharger collector were made in accordance with reference 3. The values of adiabatic efficiency of the compressor up to the diffuser stations were computed by using the total-pressure readings of the diffuser surveys and the total temperature as determined in the outlet pipe. The average total pressure at any diffuser station was obtained by arithmetically averaging the pressures obtained across the diffuser passage.

The flow parameters, corrected volume flow $Q_{1t}/\sqrt{\theta}$ and specific capacity $Q_{1t}/\sqrt{\theta}D_2^2$, and the speed parameter $U/\sqrt{\theta}$ were computed according to the method of reference 6, where

Q_{1t} volume flow at inlet stagnation conditions, cubic feet per minute

θ ratio of actual inlet stagnation temperature to standard sea-level temperature

D_2 impeller discharge-tip diameter, feet

U actual impeller tip speed, feet per second

A blade-inlet angle of attack was computed at the impeller inlet root-mean-square diameter over the range of volume flows and impeller tip speeds. The angle of attack is given with reference to the mean camber line of the inducer blades and is positive when the air strikes the lower surface and negative when the air strikes the upper surface. A blade-inlet Mach number relative to the blade was also computed at the impeller inlet root-mean-square diameter and at the impeller inlet blade tip.

An index of impeller static-pressure ratios was computed by using the static-pressure measurements made along the stationary impeller shroud. This ratio index is the minimum static pressure along the shroud divided by the static pressure at the impeller inlet.

RESULTS AND DISCUSSION

A comparison of the performance of impellers A, B, C, and D is presented to show the effects on performance of reducing the impeller tip diameter with consequent increase in the impeller angular velocity for a given impeller tip speed. The comparative performance is presented on a basis of adiabatic efficiency, pressure coefficient, and volume flow. An analysis of the volume-flow limitations of the compressor is presented. This analysis indicates what part of the compressor system limits the volume-flow capacity and shows the nature of the flow restriction. The use of impeller blade-inlet relative Mach number as an impeller design parameter is discussed.

Comparison of Performance

Adiabatic efficiency. - The over-all adiabatic efficiencies for impellers A, B, and C in conjunction with the vaneless diffuser are shown in figure 4. With each successive reduction in impeller tip diameter and consequent increase in angular velocity for a given impeller tip speed, the compressor adiabatic efficiency increases. At the high impeller tip speeds the increase in adiabatic efficiency is prevalent over the entire range of corrected volume flows; whereas at the low tip speeds the improvement in the efficiency occurs over a volume-flow range from maximum flow to

volume flows slightly below the peak-efficiency point. At an impeller tip speed of 800 feet per second, the difference in peak adiabatic-efficiency values for impellers A, B, and C is negligible, peak efficiency being 0.78. At an impeller tip speed of 1200 feet per second, the peak adiabatic efficiency increases from 0.66 to 0.72. Peak adiabatic efficiency occurs at approximately the same volume flows at the lower impeller tip speeds. At the high impeller tip speeds, the volume flow at peak adiabatic efficiency increases slightly for each reduction in impeller tip diameter.

The adiabatic efficiencies determined from total-pressure measurements in the diffuser at diameters corresponding to $1\frac{1}{2}$ impeller diameters are shown in figure 5. At the low impeller tip speeds, the peak adiabatic efficiencies are the same for the three impellers. An improvement in the efficiency with reduction of tip diameter is prevalent at the high corrected volume flows. At the high impeller tip speeds, the efficiency curves as established at the diffuser stations have the same relative characteristics as the curves of over-all efficiency. In general, the trends established from these diffuser surveys correlate with the corresponding over-all performance characteristics and indicate that the characteristics determined from outlet-pipe measurements are adequate to establish the relative merits of the three impellers.

Adiabatic-efficiency curves for impeller D are shown in figure 6. The efficiencies are based on diffuser pressure measurements at a diffuser diameter corresponding to $1\frac{1}{2}$ impeller tip diameters. Because of the extreme change in direction of the diffuser passage at the impeller discharge, diffuser mixing losses may cause the absolute values of efficiency to be in error; these losses are insufficient, however, to nullify comparison of performance over the range of impeller tip speeds. The curves show a similarity over the speed range. An increase of impeller tip speed from 700 to 1000 feet per second resulted in a 3-point drop in peak adiabatic efficiency. The shift of peak efficiency to high corrected volume flows for each respective increase in speed corresponds to the design volume flow of impeller D, which was based on a constant volume flow per revolution.

The efficiency curves for impeller D are very similar to the characteristic efficiency curves of several inducers that were tested and rated as compressors. (See reference 2.) Figure 7(a) shows the relation of peak adiabatic efficiency and angular velocity for impeller D and for a 2.00-inch-deep inducer reported in reference 2. For the range of angular velocities covered, the general trend of performance was for the inducers to maintain their efficiency over

the speed range. Figure 7(b) shows the relation of peak adiabatic efficiency for impellers A, B, and C with angular velocity. With each respective decrease in impeller diameter and consequent increase in the amount of ideal work of compression resulting from increased angular accelerations, the performance curves flatten and more closely resemble characteristic inducer performance curves. For this type of impeller, an increase in the amount of work of compression resulting from the angular acceleration in the impeller with respect to the larger component of work of compression resulting from the Coriolis acceleration in the impeller seemed to improve the impeller adiabatic efficiency.

Pressure coefficient. - The over-all pressure coefficients for the three impellers A, B, and C are shown in figure 8. Increasing the impeller angular velocities while maintaining constant impeller tip speeds resulted in an improved pressure coefficient over the range of impeller tip speeds covered. These curves indicate the same relative performance characteristics as do the curves of adiabatic efficiency. The largest change in peak pressure coefficient occurs at the higher tip speeds; at an impeller tip speed of 1200 feet per second, the peak pressure coefficient is increased 6 points. The ratio of pressure coefficient to adiabatic efficiency increases with each respective decrease in impeller diameter and indicates corresponding increases in the addition of energy to the air by the impeller.

No pressure coefficients are presented for impeller D because it has a varying discharge diameter, a condition that makes pressure coefficient an unsuitable parameter for comparison of performance.

Volume flow. - With each successive reduction in impeller diameter, an increased volume flow through the compressor was obtained. As shown in figure 4 this increased volume flow was prevalent over the range of impeller tip speeds covered by this investigation. The range of operation, defined by the ratio of maximum to minimum volume flow, was decreased as the impeller diameter was decreased. The increased volume flow for each reduction in impeller diameter resulted in very large increases in the specific capacity of the respective impellers. A comparison of specific capacity for the three impellers at an impeller tip speed of 1200 feet per second is shown in figure 9. A maximum specific capacity of 11,500 cubic feet per minute per square foot was obtained with impeller C as compared with 8600 cubic feet per minute for impeller B and 6700 cubic feet per minute for impeller A.

A flow restriction resulting from sonic velocities in the compressor was never reached with impeller D because of the limitations of the air-exhauster system used; therefore a comparison of

maximum volume flows between impeller D (fig. 6) and impellers A, B, and C is unjustified.

Complete information concerning the performance characteristics for the most efficient of the three impellers is given for impeller C in figure 10, in which the over-all total-pressure ratios P_{2t}/P_{1t} for corrected impeller tip speeds of 778, 955, 1071, and 1166 feet per second are plotted against corrected volume flow and specific capacity with contours of over-all adiabatic efficiencies.

Analysis of Volume-Flow Limitations

Previous investigations of impellers (reference 1) have shown that the volume-flow capacity of the inducer section is reflected in the volume-flow capacity of the impeller. Results from the present investigations made at constant angular speeds for each of impellers A, B, and C (fig. 11(a)) show the maximum volume flow of the impeller to be independent of the impeller diameter and impeller tip speed but to be dependent upon the impeller angular velocity. Figure 11(b) shows a plot of maximum volume flow against impeller angular velocity. The maximum volume flow varies linearly with impeller angular velocity. Inasmuch as the maximum volume flows were dependent upon the impeller angular velocities, the conditions of sonic velocity in the compressor system and the resulting flow restriction must have occurred in the inducer section.

Blade-inlet angle of attack is plotted against Mach number relative to the blade-inlet at a root-mean-square blade diameter in figure 12. For a range of impeller tip speeds and for impellers A, B, and C, values of a static-pressure-ratio index are plotted as contours. This index is a ratio of the minimum static pressure measured along the stationary impeller shroud to the static pressure at the impeller blade inlet. The heavy solid line drawn through the maximum Mach number and maximum negative angle of attack represents the maximum-volume-flow line for the range of impeller tip speeds presented. This line presents a linear relation between the blade-inlet angle of attack and blade-inlet relative Mach number with respect to the flow restriction in the inducer section. An examination of the static-pressure-ratio index shows that a critical value of approximately 0.50 existed for each of the impellers and that the maximum-flow line and the critical-pressure line are approximately the same. In all cases the critical-pressure drops occurred in the inducer section. This phenomenon indicates that the flow was restricted when a critical-pressure drop occurred in the inducer section and that,

with an increased blade-inlet relative Mach number, the negative blade-inlet angles of attack at which the critical pressure drop occurred decreased.

Use of Blade-Inlet Relative Mach Number as a Design Parameter

The comparison of the performance of impellers A, B, and C has shown that successive increases in the ratio of impeller inlet-tip diameter to impeller discharge-tip diameter resulted in considerable improvement in the impeller performance. For each increase in the ratio of impeller inlet-tip to discharge-tip diameter, there was a corresponding increase in the impeller angular velocity required for operation at a given impeller tip speed. Increased impeller angular velocities resulted in increased Mach numbers relative to the impeller blade inlet.

Hawthorne (reference 7) derived a theoretical expression relating the mass flow rate and the impeller tip, eye, and hub dimensions with the Mach number and the tip speed. He plotted the expression

$$\frac{1}{1 - h^2/e^2} \frac{W}{D^2} \left(\frac{U}{1400}\right)^2 \text{ against } \frac{eU}{1400} \text{ for four values of M, where}$$

h ratio of inside diameter of eye (hub diameter) to impeller tip diameter

e ratio of outside diameter of eye to impeller tip diameter

W mass flow rate

D impeller tip diameter

U impeller tip speed

M tip Mach number

This curve from figure 5 of reference 7 is reproduced as figure 13 with test points for impeller C added. Some of these data points show that the impeller was operating in a transonic range relative to the inlet blade tip and that a maximum Mach number of 1.03 was reached. The blade-inlet Mach number relative to the inlet blade tip has been used as a design parameter on the basis that high Mach numbers at the impeller inlet would be detrimental to the impeller

performance. Campbell and Talbert (reference 8) recommended that, for impellers of the radial-bladed type discussed in reference 8, the maximum blade-inlet relative Mach number should be below 0.75. Although impeller C was operating in a transonic range relative to the impeller inlet blade tip, this impeller showed considerable improvement in adiabatic efficiency, pressure coefficient, and volume-flow capacity as compared with impellers A and B, which operated at lower blade-inlet Mach numbers. For operation at transonic conditions at the impeller inlet, any detrimental effects on impeller performance resulting from high inlet Mach numbers appear small as compared with the desirable performance effects that were obtained by increasing the impeller angular velocity and consequently increasing the amount of work of compression resulting from the angular acceleration of the air in the impeller.

SUMMARY OF RESULTS

The effect on the performance of increasing the angular velocity of an impeller and consequently increasing the amount of work of compression resulting from the angular acceleration of the air in the impeller was investigated for four impellers in combination with a vaneless diffuser in a variable-component supercharger test rig over a range of actual tip speeds from 800 to 1300 feet per second. Impellers A, B, and C were also tested at two constant impeller angular velocities. Impellers B and C were made by successive reduction in the discharge-tip diameter of impeller A; impeller D was the inducer section alone. The following results were obtained:

1. The impeller adiabatic efficiency, pressure coefficient, and volume-flow capacity were improved when the amount of work resulting from the angular acceleration was increased with respect to the work of compression resulting from the increased radius of rotation of the impeller.

2. The volume-flow capacity of the impeller was independent of impeller diameter and impeller tip speed but dependent upon the impeller angular velocity. The relation between maximum volume flow and the impeller angular velocity was linear.

3. The volume-flow restriction in the compressor occurred in the inducer section. The flow was restricted when a critical pressure drop occurred in the inducer section, and with an increased impeller blade-inlet relative Mach number the negative blade-inlet angles of attack at which the critical pressure drop occurred decreased.

4. Any detrimental effects on impeller performance resulting from transonic velocities relative to the impeller inlet blade tip were small as compared with the desirable performance effects that were obtained by increasing the impeller angular velocity and consequently increasing the amount of work of compression resulting from the angular acceleration of the air in the impeller.

Aircraft Engine Research Laboratory,
National Advisory Committee for Aeronautics,
Cleveland, Ohio, October, 11, 1946.

REFERENCES

1. Ritter, William K., Ginsburg, Ambrose, and Beede, William L.: Performance Comparison of Two Deep Inducers as Separate Components and in Combination with an Impeller. NACA ARR No. E5J03, 1945.

2. Ritter, William K., and Johnsen, Irving A.: Preliminary Investigation of Deep Inducers as Separate Supercharger Components. NACA ARR No. E5I28, 1945.

3. Ellerbrock, Herman H., Jr., and Goldstein, Arthur W.: Principles and Methods of Rating and Testing Centrifugal Superchargers. NACA ARR, Feb. 1942.

4. NACA Subcommittee on Supercharger Compressors: Standard Procedures for Rating and Testing Centrifugal Compressors. NACA ARR No. E5F13, 1945.

5. Ebaugh, N. C., and Whitfield, R.: The Intake Orifice and a Proposed Method for Testing Exhaust Fans. A.S.M.E. Trans., PTC-56-3, vol. 56, no. 12, Dec. 1934, pp. 903-911.

6. NACA Subcommittee on Supercharger Compressors: Standard Method of Graphical Presentation of Centrifugal Compressor Performance. NACA ARR No. E5F13a, 1945.

7. Hawthorne, William R.: Factors Affecting the Design of Jet Turbines. SAE Jour. (Trans.), vol. 54, no. 7, July 1946, pp. 347-357.

8. Campbell, Kenneth, and Talbert, John E.: Some Advantages and Limitations of Centrifugal and Axial Aircraft Compressors. SAE Jour. (Trans.), vol. 53, no. 10, Oct. 1945, pp. 607-618.

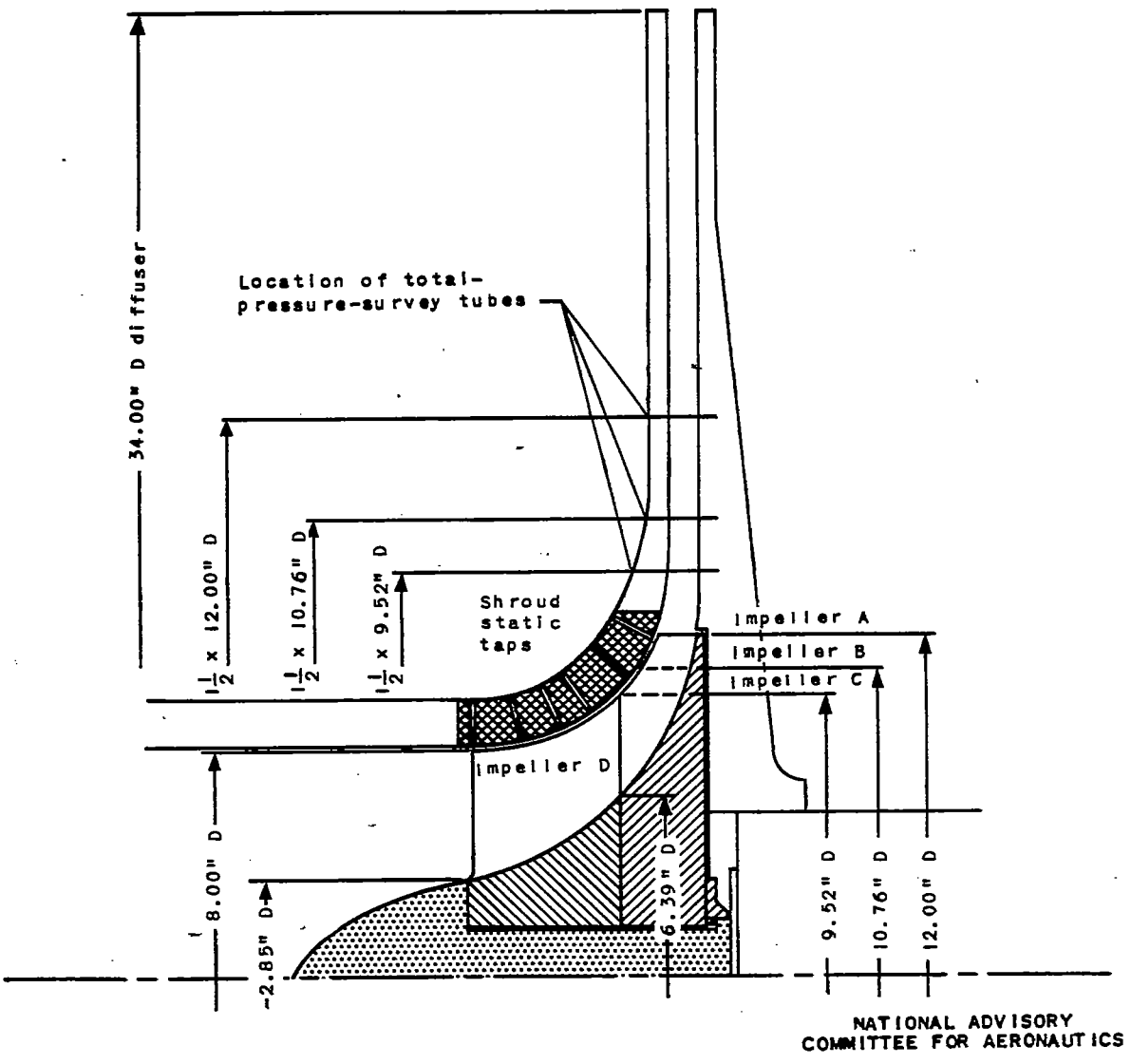

Figure 1. - Cross-sectional sketch showing design details of impellers A, B, C, and D and instrumentation in diffuser and along stationary shroud.

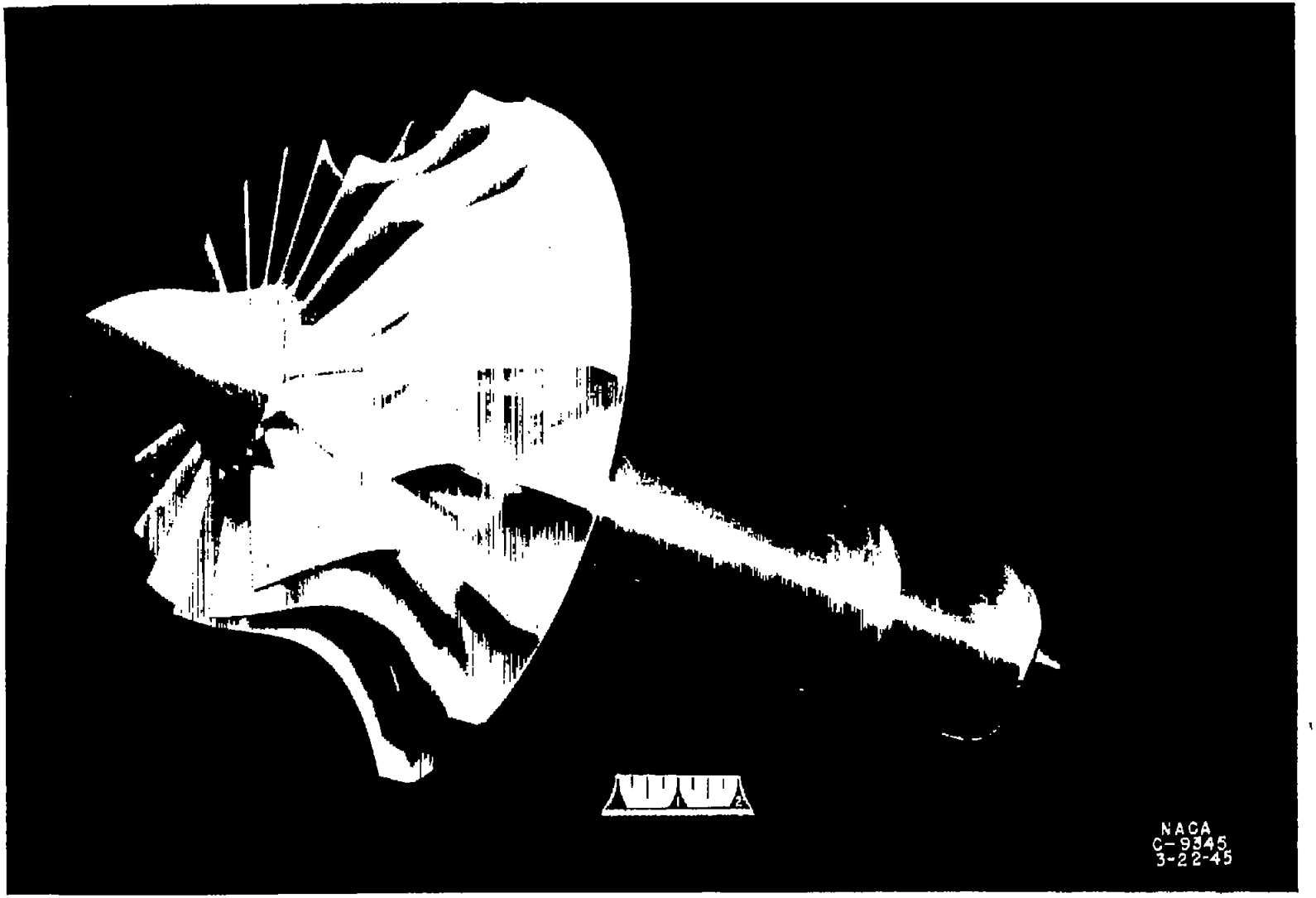

Figure 2. Impeller A.

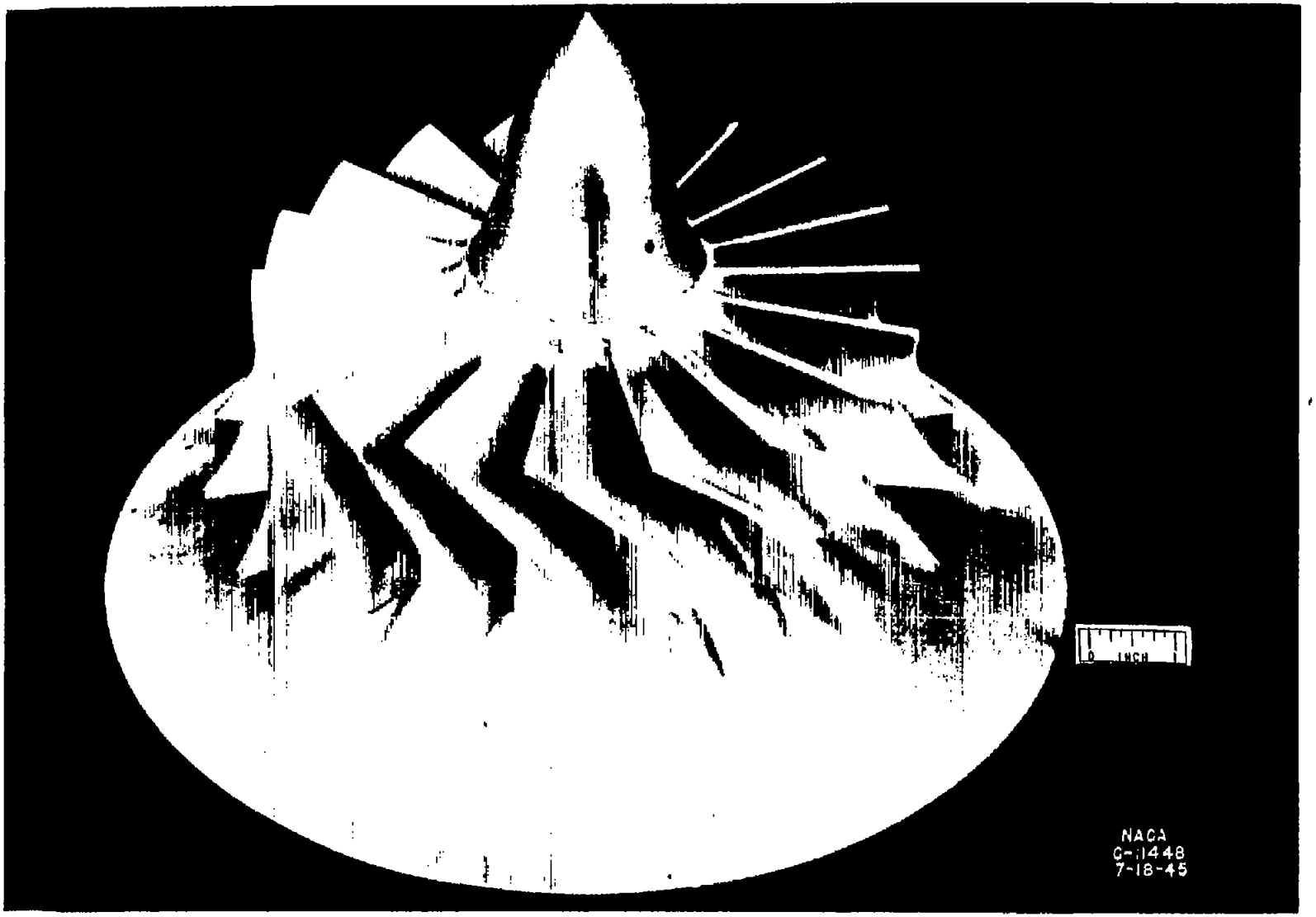

Figure 3. Impeller D.

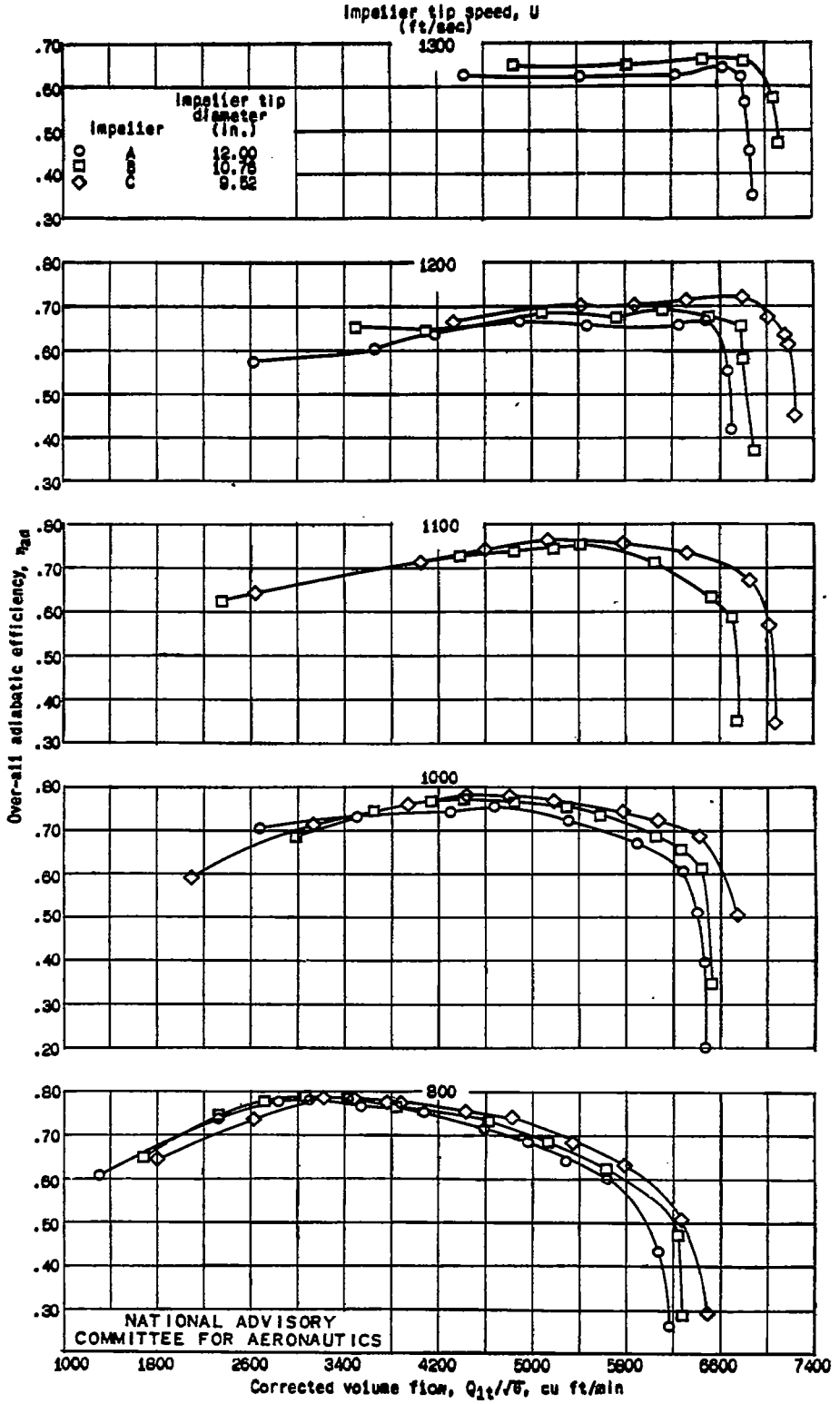

Figure 4. - Over-all adiabatic efficiencies of impellers A, B, and C.

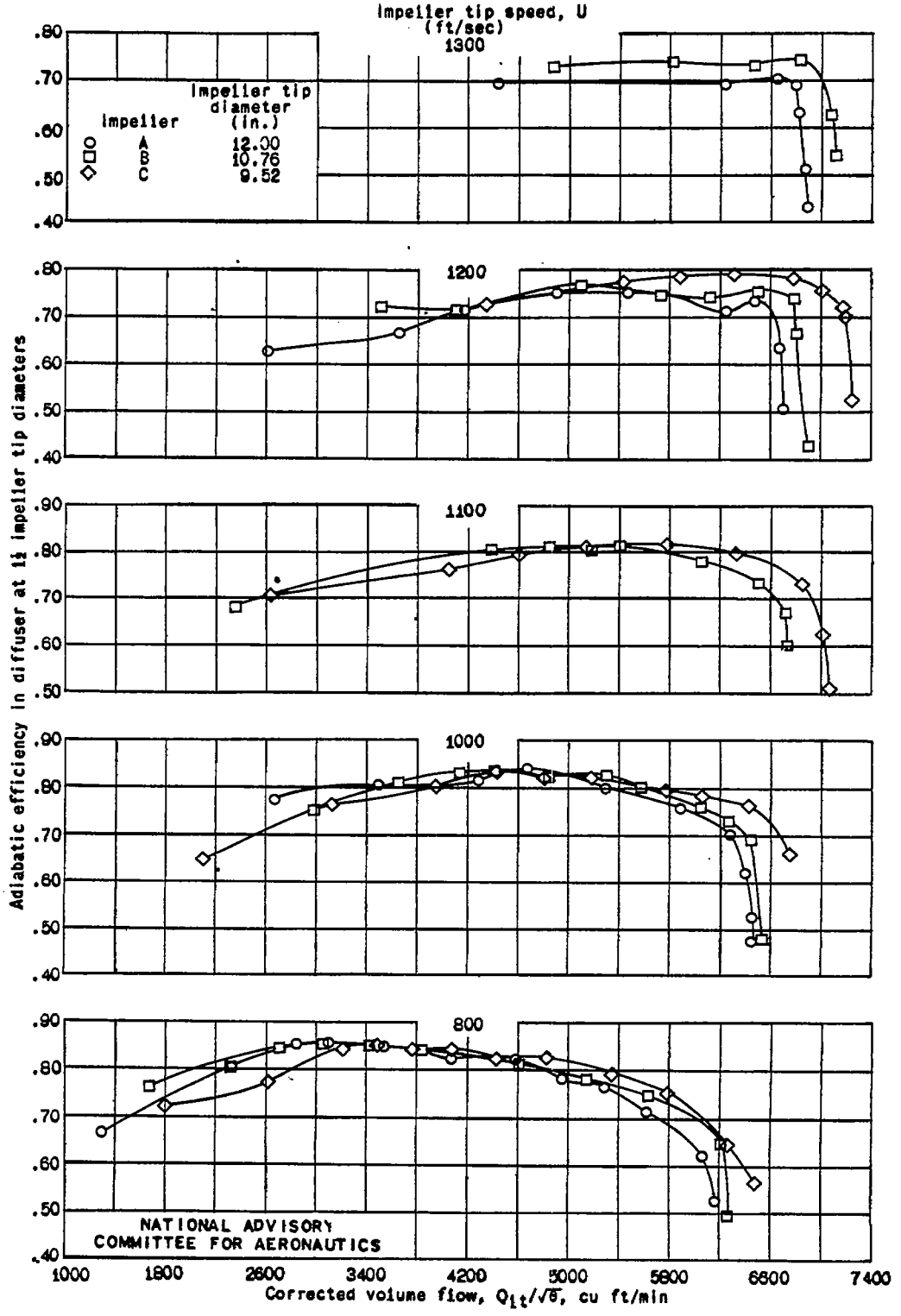

Figure 5. - Adiabatic efficiencies of impellers A, B, and C as determined in the diffuser passage.

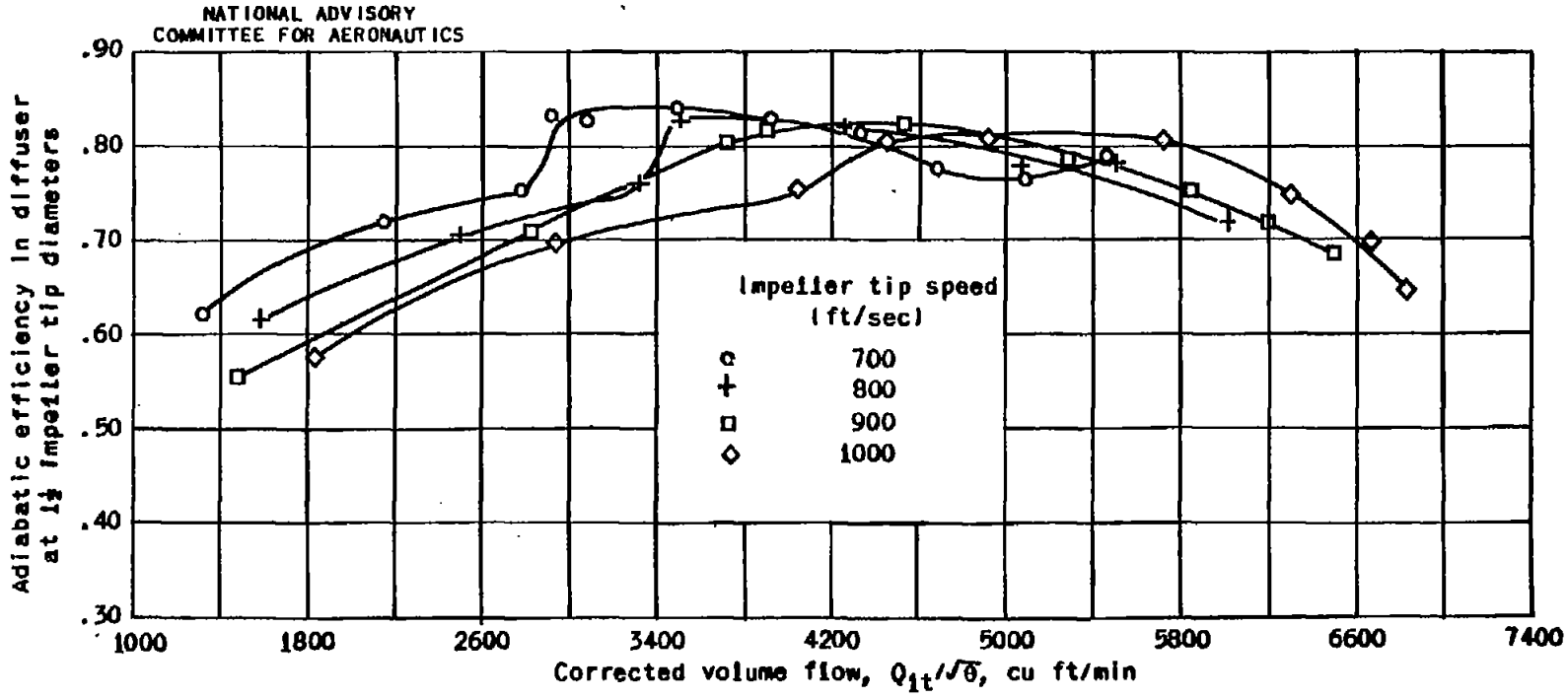

Figure 6. – Adiabatic efficiencies of impeller D.

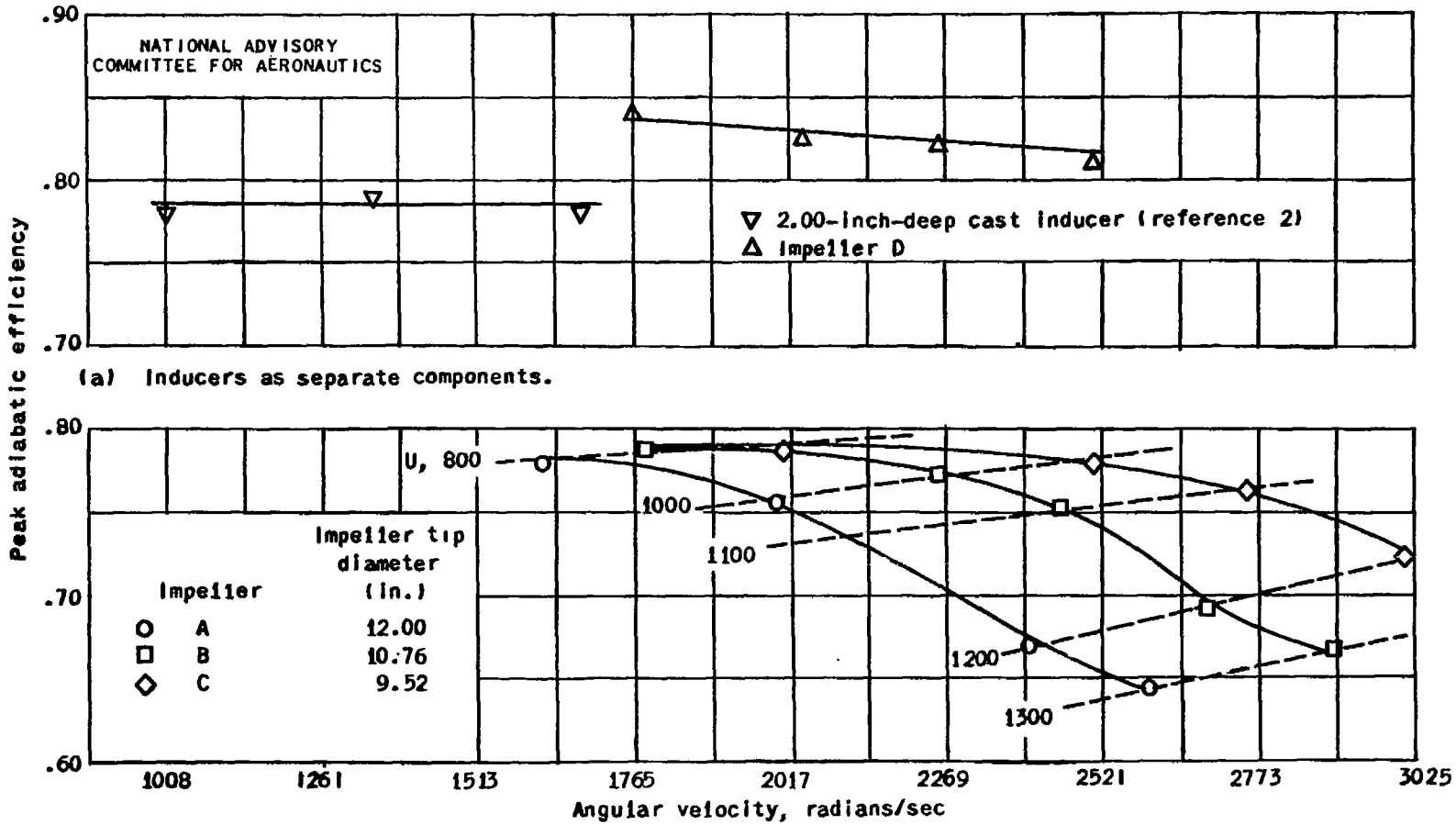

Figure 7. – Comparison of peak adiabatic efficiencies for impellers A, B, C, and D and a 2.00-inch-deep cast inducer.

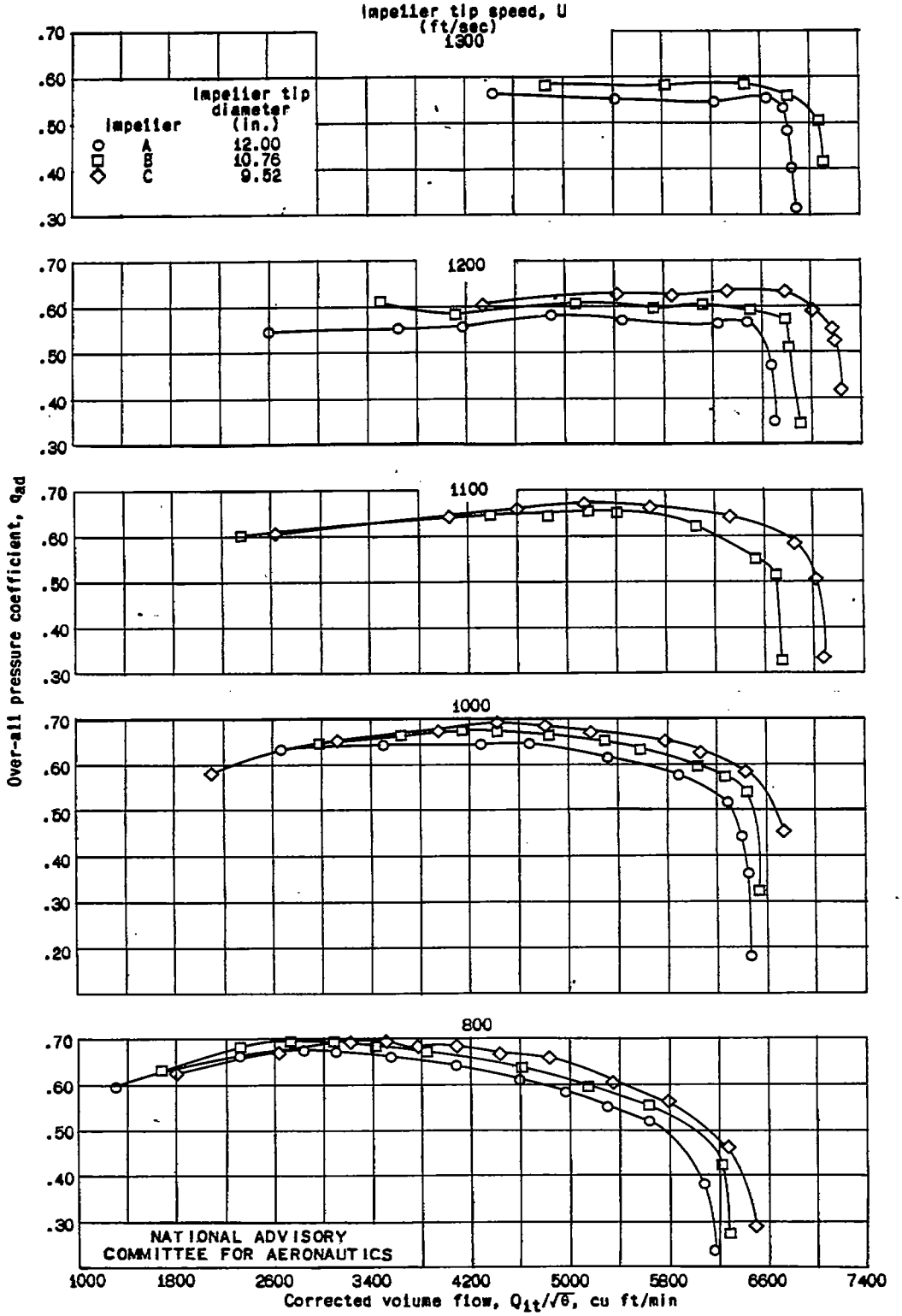

Figure 8. - Over-all pressure coefficients of impellers A, B, and C.

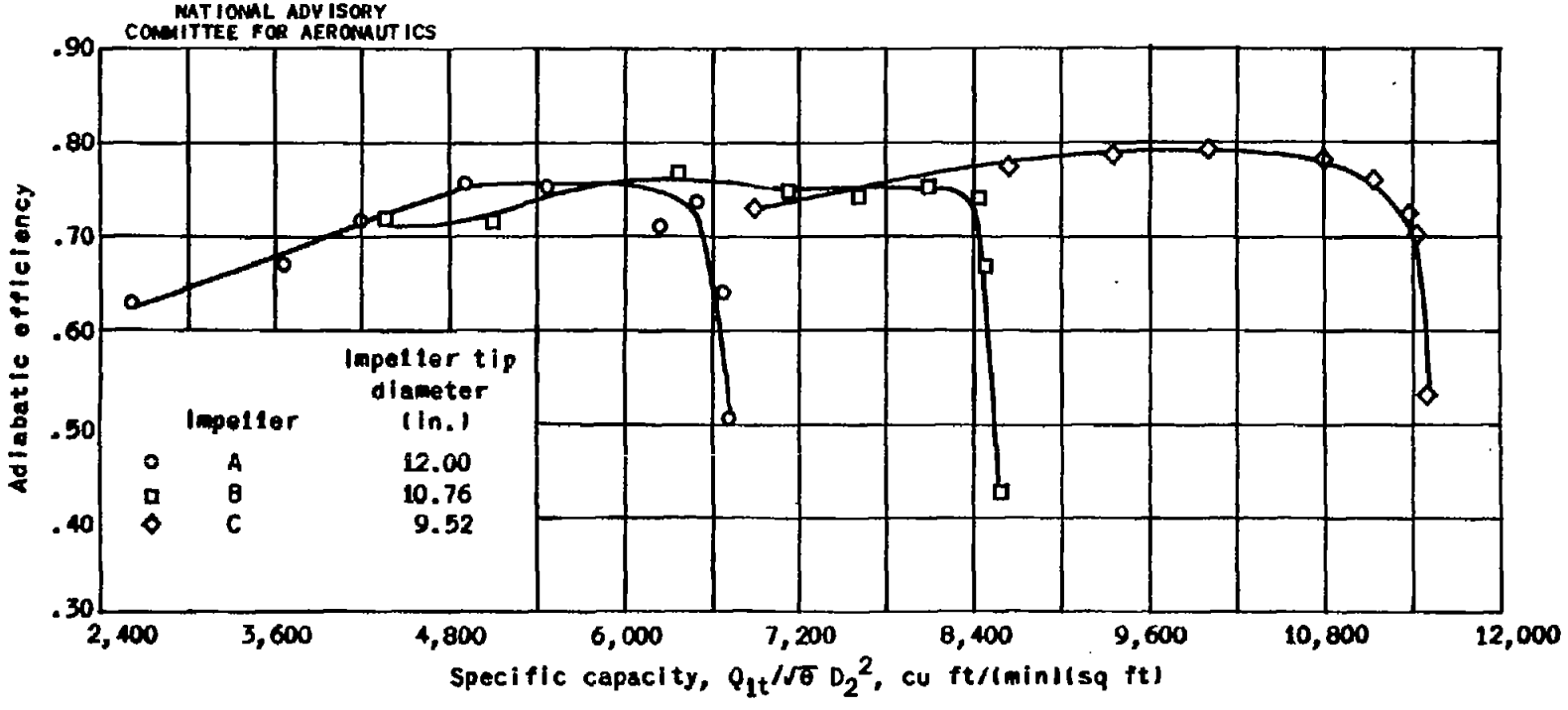

Figure 9. – Specific capacity of impellers A, B, and C at impeller tip speed of 1200 feet per second.

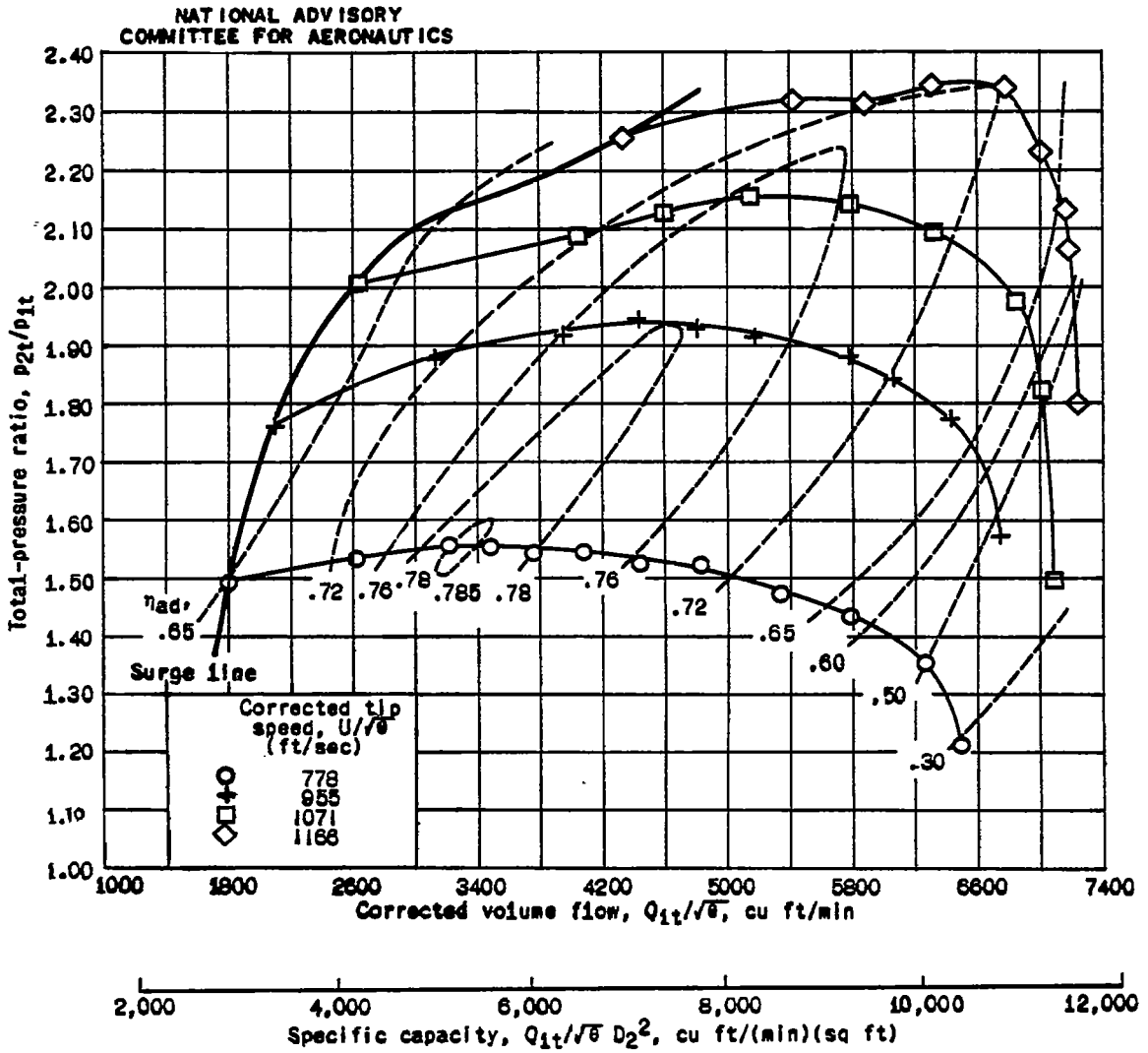

Figure 10. - Over-all performance characteristics of impeller C.

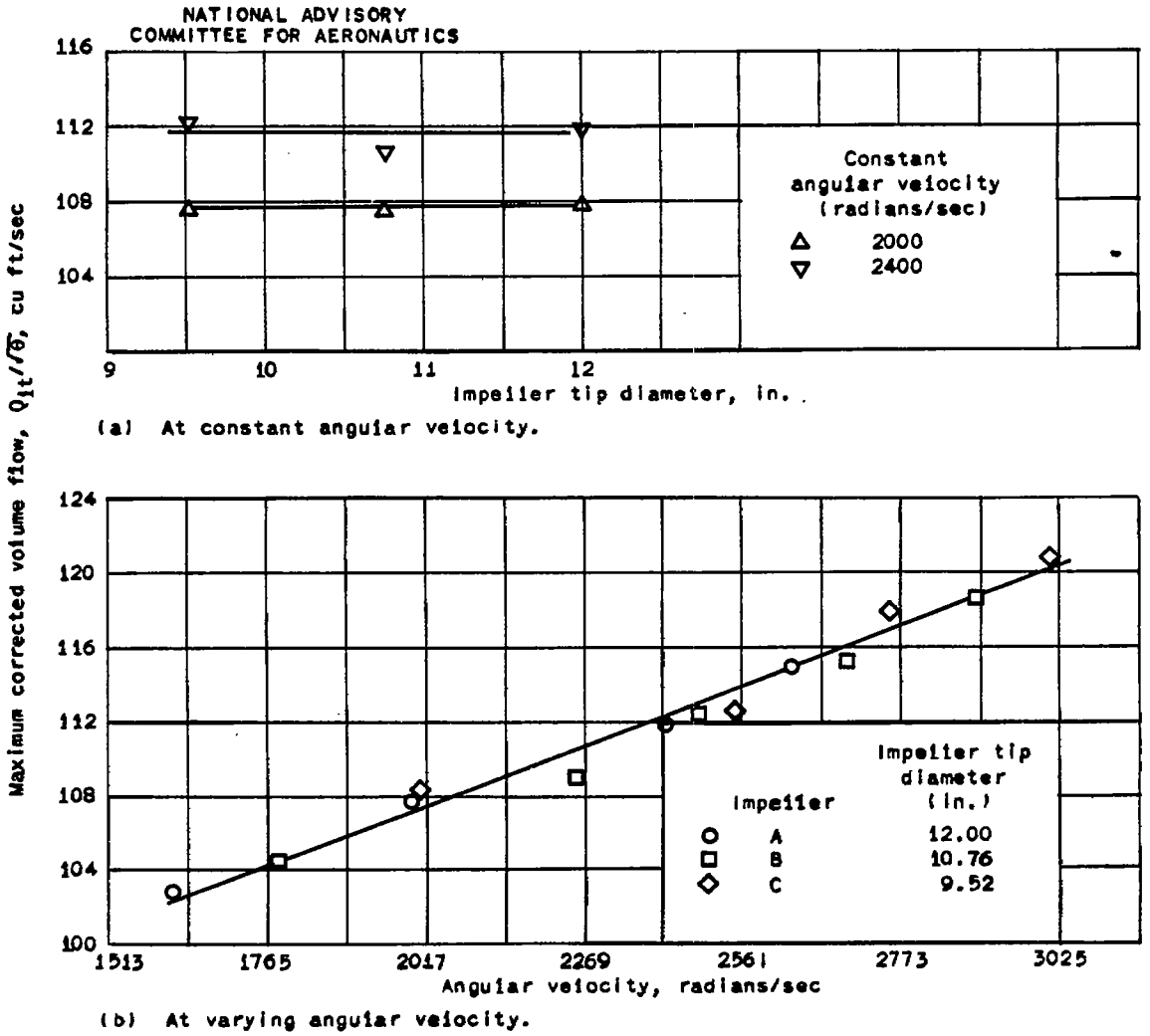

Figure 11. - Correlation of maximum volume flow of impellers with impeller angular velocity.

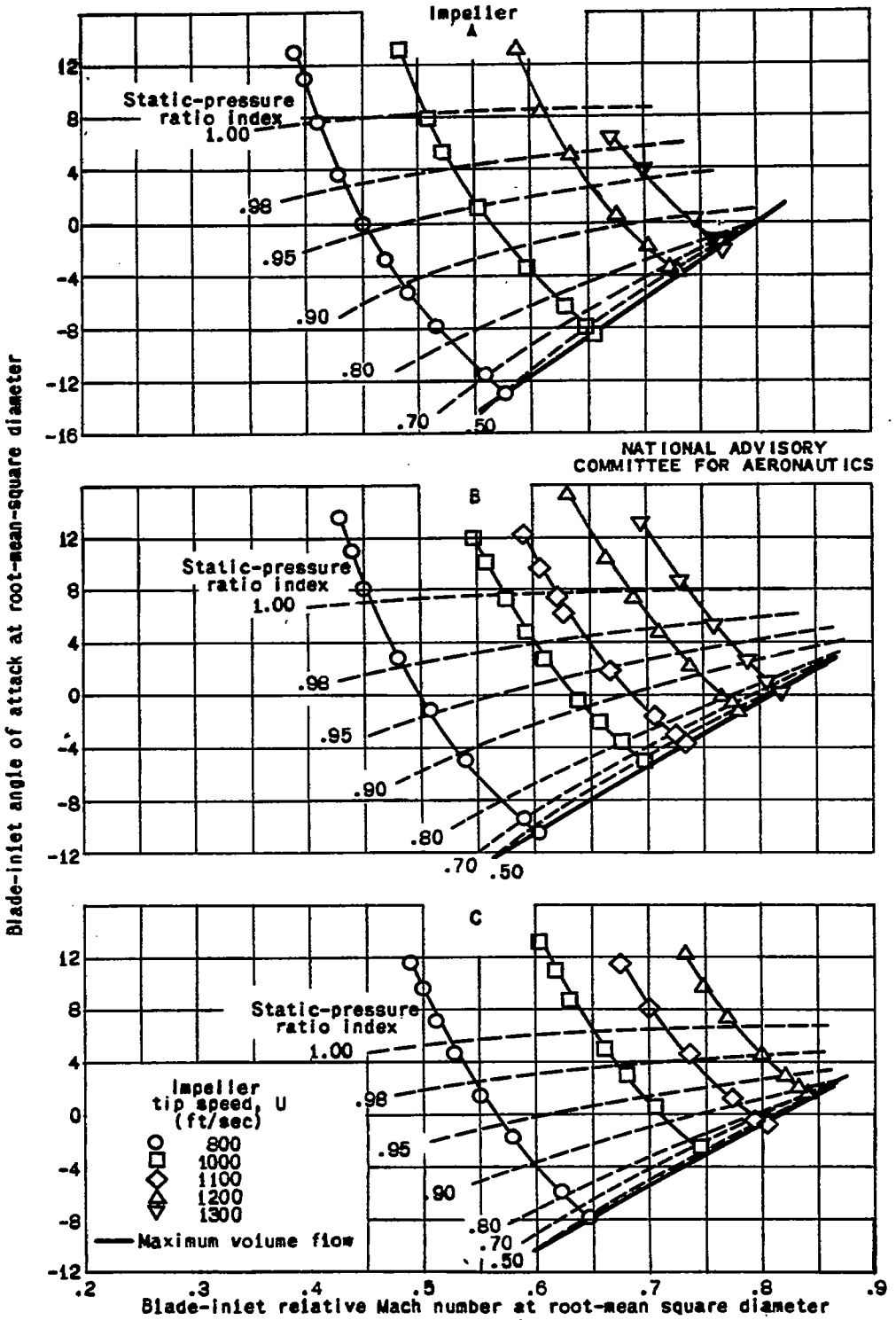

Figure 12. - The relation of maximum volume flow of impellers A, B, and C with blade-inlet angle of attack, blade-inlet relative Mach number, and measured static-pressure drop along stationary shroud. (Static-pressure-ratio index is the ratio of the minimum static pressure along the impeller stationary shroud to the static pressure at the impeller inlet.)

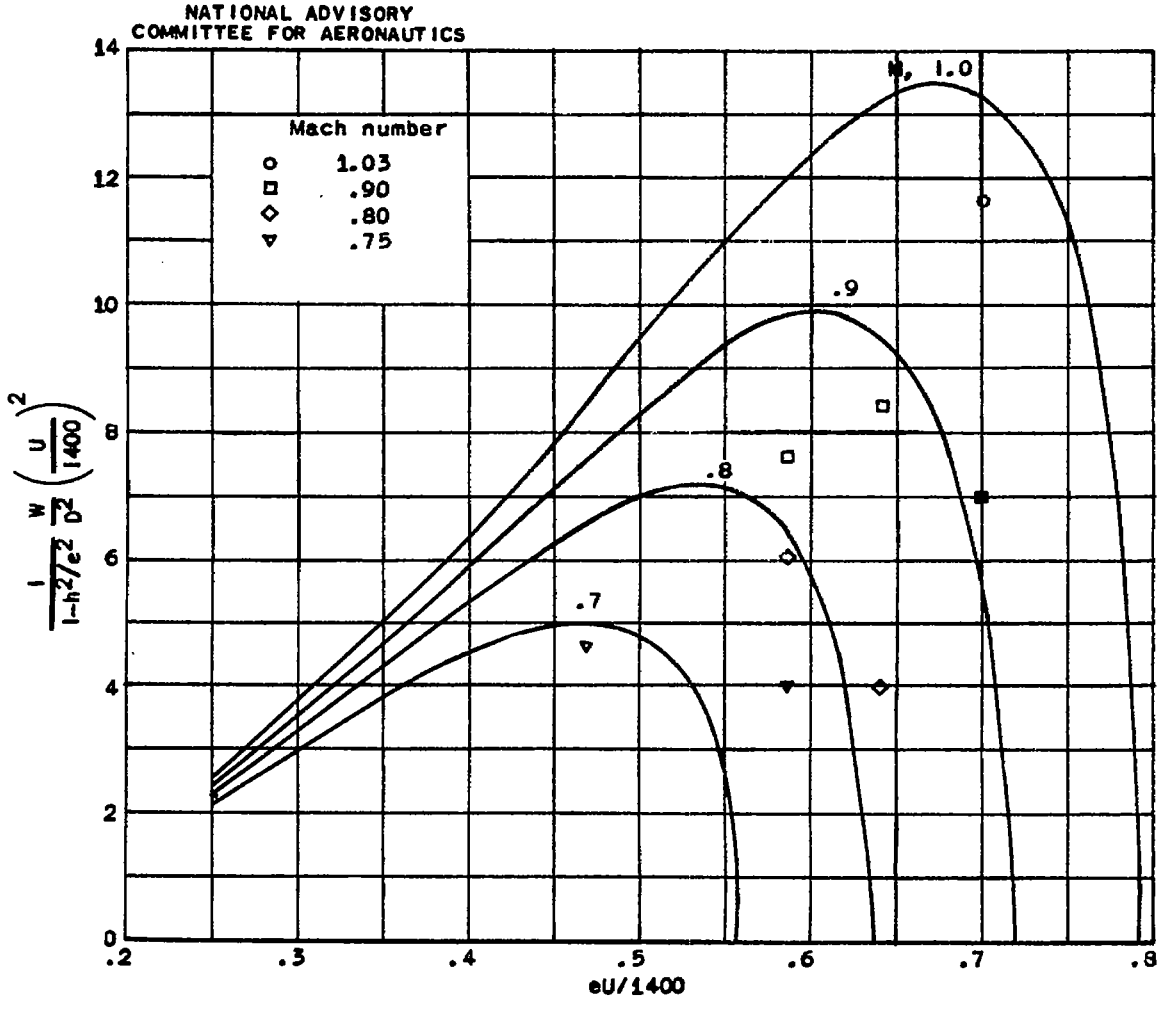

Figure 13. - Theoretical expression of impeller volume-flow capacities taken from reference 7 (fig. 5) with test points for impeller C.